



Breast Imaging Findings of Microcalcifications in Ductal Carcinoma in Situ and Their Correlations with Pathological and Biological Features

Eun Ji Lee ¹ and Yun-Woo Chang ^{1,*}

¹Department of Radiology, Soonchunhyang University Seoul Hospital, Seoul, Republic of Korea

*Corresponding author: Department of Radiology, Soonchunhyang University Seoul Hospital, 04401, Seoul, Republic of Korea. Email: ywchang@schmc.ac.kr

Received 2021 May 19; Revised 2021 September 24; Accepted 2021 September 26.

Abstract

Background: Mammography (MMG) is the primary screening tool for breast cancer, as microcalcifications are the most common MMG finding in ductal carcinoma in situ (DCIS). The use of high-frequency transducers facilitates the visualization of calcifications on ultrasonography (USG), especially in patients with dense breasts and cancer symptoms. Although a correlation has been reported between the imaging features of DCIS and pathological features, few studies have focused on multiple imaging modalities.

Objectives: To evaluate the correlation of DCIS microcalcifications in breast imaging with pathological and biological features.

Patients and Methods: The MMG and USG findings of 125 lesions detected in 123 patients, diagnosed with pure DCIS, were retrospectively reviewed according to the breast imaging-reporting and data system (BI-RADS). The USG and comparable MMG findings of microcalcifications were divided into three groups: group 1 (MMG negative, USG negative), group 2 (MMG positive, USG negative), and group 3 (MMG positive, USG positive). The pathological findings (nuclear grade and comedo necrosis) and biological features [estrogen (ER) positive group, human epidermal growth factor receptor 2 (HER2) positive group, triple negative group, and Ki-67 index] were compared with the MMG and USG features using Chi-square test.

Results: Microcalcifications were observed on MMG in 83 (66.4%) DCIS lesions. Positive microcalcifications on MMG were significantly associated with a high nuclear grade ($P = 0.001$) and comedo necrosis ($P = 0.001$). Positive microcalcifications on MMG were significantly associated with ER negativity ($P = 0.023$), HER2 positivity ($P = 0.002$), and increased Ki-67 index ($P = 0.001$). There were 62 lesions (49.6%) without microcalcifications on USG (group 1 and group 2), while there were 63 (50.4%) lesions with microcalcifications on USG (group 3). Positive microcalcifications on MMG were significantly associated with ER-negative group ($P = 0.023$), HER2-positive group ($P = 0.002$), and increased Ki 67 index ($P = 0.001$).

Conclusion: Based on the present results, DCIS microcalcifications detected via imaging were significantly associated with poor prognostic pathological factors, such as a high nuclear grade and comedo necrosis, as well as poor prognostic biological factors, including ER negativity, HER2 positive group, and a high Ki-67 index.

Keywords: Breast, Ductal Carcinoma in Situ, Mammography, Sonography

1. Background

Ductal carcinoma in situ (DCIS) of the breast is a clinically, radiologically, and genetically heterogeneous spectral group of diseases. It is characterized by a malignant proliferation of ductal epithelial cells within the terminal duct lobular unit, without invasion of the basement membrane. Although DCIS is an obligate precursor of invasive ductal carcinoma, almost 30 to 50% of all untreated DCIS cases progress into invasive ductal carcinoma, according to previous reports (1-4).

Nevertheless, all patients diagnosed with DCIS are commonly treated for invasive carcinoma, because there are

no reliable predictive markers of disease progression (3). Mammography (MMG) is the primary screening tool for breast cancer, as microcalcifications are the most common MMG finding of DCIS (5, 6). Moreover, advances in technology and application of high-frequency transducers have facilitated the visualization of calcifications on ultrasonography (USG), especially in patients with dense breasts and cancer symptoms (7, 8).

Microcalcifications with suspicious features are associated with specific pathological features, such as a high nuclear grade and human epidermal growth factor receptor 2 (HER2) overexpression (9, 10). A higher nuclear grade, comedo necrosis, and a solid or cribriform archi-

tectural pattern are known to increase the risk of DCIS or invasive tumor recurrence in patients undergoing a breast-conserving surgery (11, 12). Moreover, estrogen receptor (ER), progesterone receptor (PR), C-erb B2 oncogene (HER2) expression, and Ki-67 proliferation index are well-established biomarkers for the prognosis of DCIS (13, 14). The ER status and HER2 status are usually maintained when DCIS progresses into invasive cancer, which specificity suggests the evolution of tumor subtype in breast cancer (15). HER2 has been considered as an important prognostic factor in invasive cancer, correlated with the prognosis of DCIS (16, 17). The HER2 status and Ki-67 index are prognostic factors, predicting the recurrence of DCIS after a breast-conserving surgery (18, 19).

A correlation has been reported between the imaging features of DCIS and pathological features in the literature, while few studies have focused on multiple imaging modalities (20-23). Therefore, this study aimed to investigate the correlation between the imaging and pathological features of pure DCIS by examining microcalcifications on MMG and USG images.

2. Objectives

This study aimed to investigate the correlation between the imaging and pathological features of pure DCIS by investigating microcalcifications on MMG and USG.

3. Patients and Methods

3.1. Patients

This retrospective study was approved by the Institutional Review Board (IRB), and the requirement for obtaining informed consent was waived. From January 2009 to January 2019, we retrospectively reviewed 156 consecutive patients with pathologically diagnosed DCIS, who had undergone MMG and USG in the last month. Thirty-three patients were excluded from the study, while there were two cases of bilateral lesions. Finally, a total of 125 lesions in 123 patients with surgically proven pure DCIS were examined in this study (Figure 1). All patients were female. Also, the average age of the participants was 52.3 years (range: 31-83 years).

3.2. Imaging Features

MMG was performed using digital mammography. The images were analyzed based on the picture archiving and communication system (PACS). Standard two-view MMG images (with an additional view if necessary) were read by two radiologists (with 18 and three years of experience in

breast imaging, respectively), without knowledge of clinical or pathological data by consensus. Besides, the morphology and distribution of calcifications were analyzed using the breast imaging reporting and data system (BI-RADS) Atlas, Fifth Edition (24).

The features of MMG were divided into two groups of visible and invisible microcalcifications. The morphology of microcalcifications was classified as follows: punctate; amorphous/coarse heterogeneous; fine pleomorphic/linear branching. Besides, their distribution was classified as follows: group, segmental, linear, regional, and diffuse. Moreover, USG was performed using a broadband 5 - 12 MHz linear array transducer (LOGIQ E9, GE, Wauwatosa, WI, USA) or a broadband 5 - 17 MHz linear array transducer (iU22, Philips, Seattle, WA, USA).

The USG analyses were carried out by the same breast imaging specialists with knowledge of MMG microcalcifications using a PACS monitor. When echogenic foci corresponded to microcalcifications on MMG, they were also diagnosed by USG. Microcalcifications were recorded by USG, according to the BI-RADS Atlas Fifth Edition (24). Positive microcalcifications on USG were classified as follows: calcification in a mass; calcification outside a mass; and intraductal calcification. USG findings of microcalcifications were divided into three groups compared with MMG microcalcifications; group 1 (MMG negative, USG negative), group 2 (MMG positive, USG negative), and group 3 (MMG positive, USG positive).

3.3. Histopathological and Immunohistochemical Analyses

The nuclear grade was divided into low, intermediate, and high based on Van Nuys Prognostic Index. The presence of comedo necrosis was also recorded, and the estrogen receptor (ER) or progesterone receptor (PR) status was defined (25). The expression of c-erb B2 oncogene (HER2) was scored from 1+ to 3+, based on the immunohistochemical analyses (26). Silver-enhanced in situ hybridization (SISH) was also used for all equivocal cases (immunohistochemical staining score, 2+), using a Ventana HER2 Dual ISH DNA Probe Cocktail (Ventana Medical Systems, Inc., USA). Moreover, the Ki-67 index was divided into low ($\leq 5\%$), intermediate (6 - 19%), and high ($\geq 20\%$), based on the percentage of positive nuclear staining of cancer cells (3, 27). All DCIS cases were classified into three groups: ER positive group (ER+, HER2-, PR + or -), HER2 positive group (HER2+, ER/PR + or -), and triple negative group (28).

3.4. Statistical Analysis

The relationships between the presence of microcalcifications on MMG and USG and the nuclear grade, comedo necrosis, ER positivity, HER2 positivity, triple negativity,

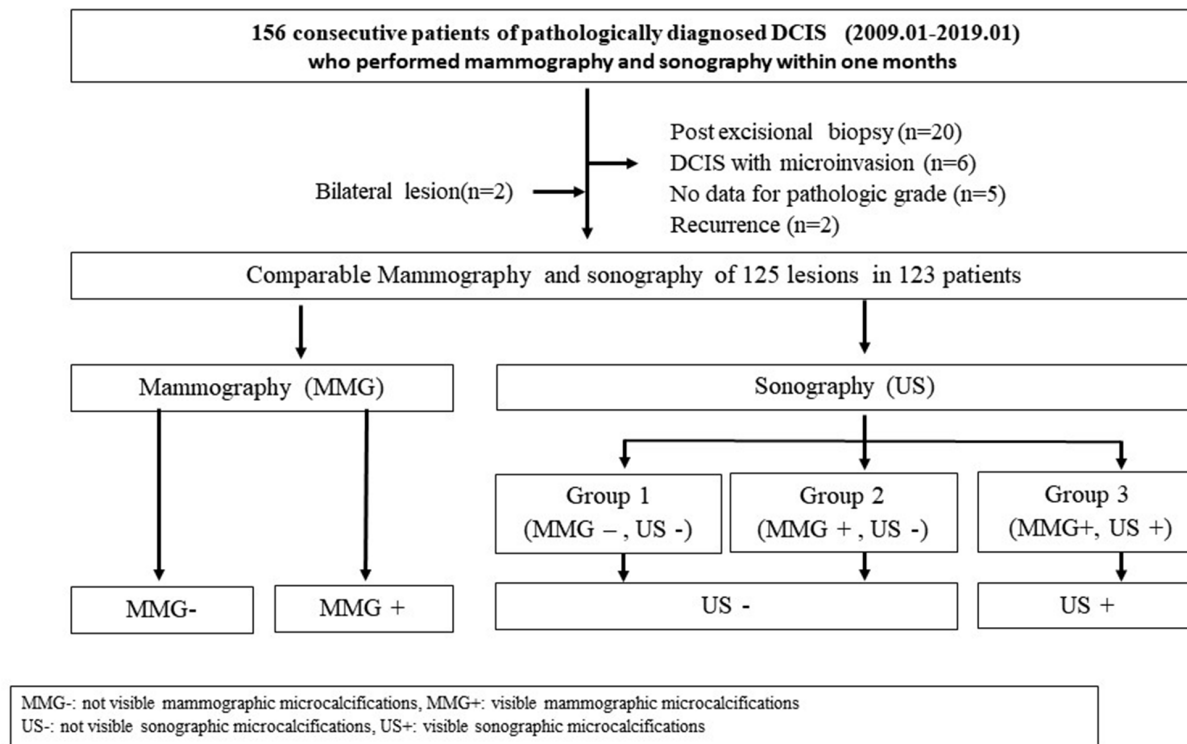


Figure 1. Patient selection

and Ki-67 index were assessed in this study. The odds ratio (OR) and 95% confidence interval (CI) were calculated. Since independent variables in the comparative analysis were nonparametric, a nonparametric analysis using chi-square test was performed. The level of statistical significance was set at $P < 0.05$. The microcalcifications detected on MMG and USG were compared in terms of nuclear grade, comedo necrosis, ER positive group, HER2 positive group by measuring the OR at 95% CI. SPSS version 20.0 (IBM SPSS Statistics, Chicago, IL, USA) was used for data analysis.

4. Results

4.1. Correlations of MMG Findings with Pathology and Immunohistochemistry

Microcalcifications were observed on MMG in 66.4% of cases (83/125). Positive MMG findings of microcalcifications were significantly associated with a high nuclear grade (OR = 15.14, 95% CI: 4.94 - 46.45, $P = 0.001$) and the presence of comedo necrosis (OR = 5.87, 95% CI: 2.60 - 13.23, $P = 0.001$) (Table 1). Moreover, positive MMG findings of microcalcifications were significantly associated with ER-negative group (the other patients except for ER positive

group, OR = 2.47, 95% CI: 1.15 - 5.27, $P = 0.023$), HER2 positive group (OR = 3.56, 95% CI: 1.61 - 7.83, $P = 0.002$), and a high Ki-67 index ($P = 0.001$) (Table 2).

4.2. Correlations of USG Findings with Pathology and Immunohistochemistry

There were 62 (49.6%) lesions with negative microcalcifications on USG (group 1 and group 2) and 63 (50.4%) lesions with microcalcifications on USG (group 3). Calcifications outside the mass were the most common finding in group 3 (34/63, 54.0%). A high nuclear grade (OR = 7.54, 95% CI: 3.37 - 16.86, $P = 0.001$) and comedo necrosis (OR = 5.38, 95% CI: 2.37 - 12.21, $P = 0.001$) were reported in group 3 (Table 3). Besides, HER2-positive group (OR: 2.41, 95% CI: 1.17 - 4.93, $P = 0.006$) and high Ki-67 index ($P = 0.001$) were significantly associated with group 3 of microcalcification findings (Figures 2 and 3). Calcifications outside the mass were also associated with ER negativity ($P = 0.017$) and HER2 positivity ($P = 0.008$) (Table 4).

5. Discussion

Based on the present results, microcalcifications detected on MMG and USG were correlated with the histo-

Table 1. Relationships Between the Morphology and Distribution of Microcalcifications on Mammography (MMG) and Histopathological Features ^a

MMG; 125 (100)		Nuclear grade; 125 (100)		P	Comedo necrosis; 125 (100)		P
		Low-intermediate; 70 (56.0)	High; 55 (44.0)		Non-comedo; 44 (35.2)	Comedo; 81 (64.8)	
Negative microcalcifications	42 (33.6)	38 (30.4)	4 (3.2)	0.001	26 (20.8)	16 (12.8)	0.001
Positive microcalcifications	83 (66.4)	32 (25.6)	51 (40.8)		18 (14.4)	65 (52.0)	
Morphology				0.771			0.878
Punctate	3 (3.6)	1 (1.2)	2 (2.4)		1 (1.2)	2 (2.4)	
Amorphous, coarse heterogeneous	32 (38.6)	14 (16.9)	18 (21.7)		7 (8.4)	25 (30.1)	
Fine pleomorphic, linear branching	48 (57.8)	17 (20.5)	31 (37.3)		10 (12.0)	38 (45.8)	
Distribution				0.796			0.350
Grouped	38 (45.8)	15 (18.1)	23 (27.7)		11 (13.3)	27 (32.5)	
Segmental	31 (37.3)	12 (14.5)	19 (22.9)		5 (6.0)	26 (31.3)	
Linear	6 (7.2)	3 (3.6)	3 (3.6)		2 (2.4)	4 (4.8)	
Regional	6 (7.2)	2 (2.4)	4 (4.8)		0 (0.0)	6 (7.2)	
Diffuse	2 (2.4)	0 (0.0)	2 (2.4)		0 (0.0)	2 (2.4)	

^a Values are expressed as No. (%).

Table 2. Association of Microcalcification Morphology and Distribution on Mammography (MMG) with Immunohistochemical Features ^{a, b}

MMG; 125 (100)	ER group; 125 (100)		P	HER2 group; 125 (100)		P	Triple negative; group 125 (100)		P	Ki-67 index; 120 (100)			P
	Negative; 69 (55.2)	Positive; 56 (44.8)		Negative; 61 (48.8)	Positive; 64 (51.62)		Negative; 121 (96.8)	Positive; 4 (3.2)		≤ 5%; 25 (20.8)	6 - 19%; 53 (44.2)	≥ 20%; 42 (35.0)	
Negative microcalcifications; 42 (33.6)	17 (13.6)	25 (20.0)	0.023	29 (23.2)	13 (10.4)	0.002	39 (31.2)	3 (2.4)	0.110	11 (9.2)	24 (20.0)	4 (3.3)	0.001
Positive microcalcifications; 83 (66.4)	52 (41.6)	31 (24.8)		32 (25.6)	51 (40.8)		82 (65.6)	1 (0.8)		14 (11.7)	29 (24.2)	38 (31.7)	
Positive microcalcifications; 83 (100)	52 (62.7)	31 (37.3)		32 (38.6)	51 (61.4)		82 (98.8)	1 (1.2)		14 (17.3)	29 (35.8)	38 (46.9)	
Morphology			0.186			0.122			0.446				0.302
Punctate; 3 (3.6)	3 (3.6)	0 (0.0)		0 (0.0)	3 (3.6)		3 (3.6)	0 (0.0)		0 (0.0)	0 (0.0)	3 (3.7)	
Amorphous, coarse heterogeneous; 32 (38.6)	17 (20.6)	15 (18.1)		16 (19.3)	16 (19.3)		31 (37.3)	1 (1.2)		6 (7.4)	13 (16.0)	11 (13.6)	
Fine pleomorphic, linear branching; 48 (57.8)	32 (38.6)	16 (19.3)		16 (19.3)	32 (38.6)		48 (57.8)	0 (0.0)		8 (9.9)	16 (19.8)	24 (29.6)	
Distribution			0.283			0.208			0.878				0.732
Grouped, 38 (45.8)	20 (24.1)	18 (21.7)		19 (22.9)	19 (22.9)		37 (44.6)	1 (1.2)		7 (8.6)	12 (14.8)	17 (21.0)	
Segmental, 31 (37.3)	23 (27.7)	8 (9.6)		8 (9.6)	23 (27.7)		31 (37.3)	0 (0.0)		4 (4.9)	14 (17.3)	13 (16.0)	
Linear, 6 (7.2)	3 (3.6)	3 (3.6)		3 (3.6)	3 (3.6)		6 (7.2)	0 (0.0)		1 (1.2)	2 (2.5)	3 (3.7)	
Regional, 6 (7.2)	4 (4.8)	2 (2.4)		2 (2.4)	4 (4.8)		6 (7.2)	0 (0.0)		2 (2.5)	1 (1.2)	3 (3.7)	
Diffuse, 2 (2.4)	2 (2.4)	0 (0.0)		0 (2.2)	2 (2.4)		2 (2.4)	0 (0.0)		0 (0.0)	0 (0.0)	2 (2.5)	

Abbreviations: ER, estrogen receptor; HER2, epidermal growth factor receptor 2.

^a Values are expressed as No. (%).

^b The available number of Ki-67 index was n = 120.

Table 3. Association of Microcalcification Classification Based on Ultrasonographic (USG) and Histopathological Features^a

USG; 125 (100)	Nuclear grade; 125 (100)		P	Comedo necrosis; 125 (100)		P
	Low-Intermediate; 70 (56.0)	High; 55 (44.0)		Non-comedo; 44 (35.2)	Comedo; 81 (64.8)	
Negative microcalcifications; 62 (49.6)	49 (38.9)	13 (11.1)	0.001	33 (26.2)	29 (23.2)	0.001
Group 1 (MMG-, USG-), 42 (33.6)	38 (30.2)	4 (4.0)		26 (20.8)	16 (12.8)	
Group 2 (MMG+, USG-), 20 (16.0)	11 (8.7)	9 (7.1)		7 (5.6)	13 (10.4)	
Positive microcalcifications; 63(50.4)						
Group 3 (MMG+, USG+); 63 (50.4)	21 (16.7)	42 (33.3)		11 (8.8)	52 (41.6)	
Positive microcalcifications (group 3); 63 (100)	21 (33.3)	42 (65.6)	0.195	11 (17.5)	52 (82.5)	0.536
Calcifications in a mass; 24 (38.1)	10 (15.9)	14 (22.2)		5 (7.9)	19 (30.2)	
Calcifications outside a mass; 34 (54.0)	11 (17.5)	23 (36.5)		6 (9.5)	28 (44.4)	
Intraductal calcifications; 5 (7.9)	0 (0.0)	5 (7.9)		0 (0.0)	5 (7.9)	

Abbreviations: MMG-, mammography-negative microcalcifications; MMG+, mammography-positive microcalcifications; USG-, ultrasonography-negative microcalcifications; USG+, ultrasonography-positive microcalcifications.

^a Values are expressed as No. (%).

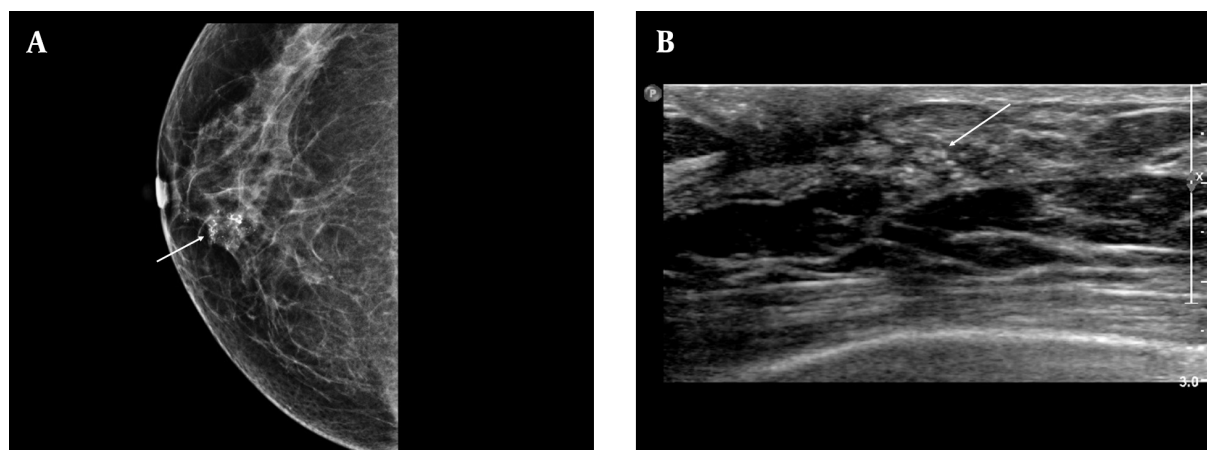


Figure 2. A, Positive microcalcifications with high-risk histological and biological markers. The mammographic (MMG) image shows grouped, coarse heterogeneous microcalcifications in the lower inner quadrant of the right breast (arrow); B, The ultrasonography (USG) image shows echogenic microcalcifications, which can be classified as group 3 mammographic (MMG) findings. Calcification outside the mass was the most common USG finding based on the breast imaging-reporting and data system (BI-RADS) (arrow). Pathology revealed poor prognostic factors, a high nuclear grade, comedo necrosis, negative ER group, positive HER2 group, and a high Ki-67 index ($\geq 20\%$).

logical features and subtypes, based on the immunohistochemical findings. In this study, 66.4% of DCIS lesions were seen as microcalcifications on MMG, which is comparable to previous studies (5, 6, 29). Pure DCIS with a high nuclear grade and comedo necrosis was significantly associated with fine linear branching, pleomorphic, and coarse heterogeneous morphologies of microcalcifications, besides the larger size of DCIS lesion on MMG (10). In the present study, visible microcalcifications on MMG were significantly associated with a high nuclear grade and comedo necrosis, which is consistent with previous studies.

Bae et al. (3) reported that HER2 levels were positively correlated with the probability of malignancy on MMG, whereas the ER status was negatively correlated with the probability of malignancy on MMG. HER2-positive DCIS commonly showed linear branching or segmental microcalcifications, while ER-positive DCIS commonly showed clustered microcalcifications. The present results showed that visible microcalcifications on MMG were significantly associated with ER negative group and HER2 positive group in DCIS. However, the morphology and distribution of microcalcifications were not significantly different be-

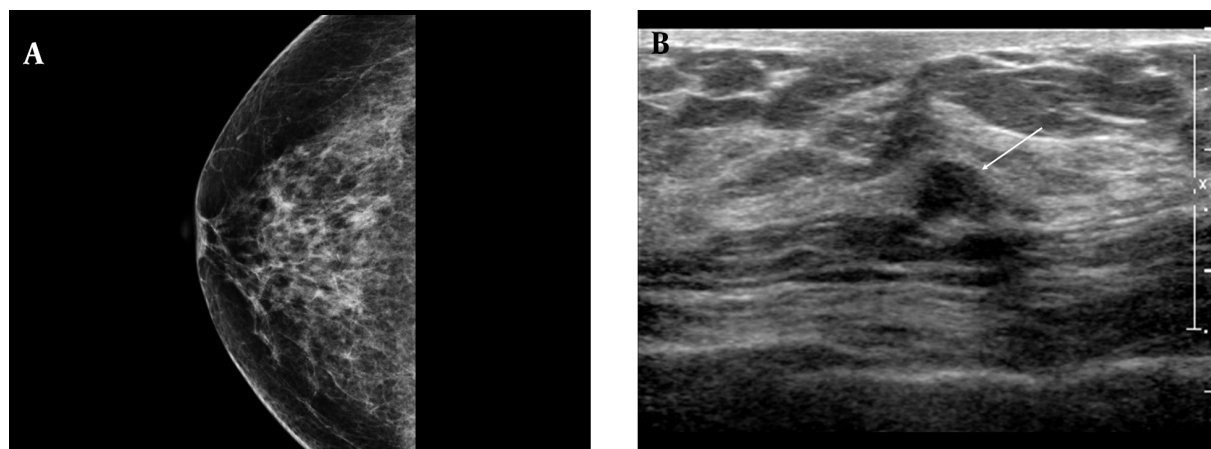


Figure 3. A, Negative microcalcifications with low-risk histological and biological markers. The mammographic (MMG) image shows a heterogeneously dense breast parenchymal composition with negative findings; B, The ultrasonography (USG) finding is classified as group 1. The USG image shows an irregular, indistinct, hypochoic mass in the right breast without microcalcifications (arrow). The pathology report revealed a low nuclear grade without comedo necrosis, positive HER2 group, and negative HER2 group, with a low Ki-67 index (< 10%).

Table 4. Association of Ultrasonographic (USG) Classification of Microcalcifications with Immunohistochemical Features^{a, b}

USG; 125 (100)	ER group; 125 (100)		P	HER2 group; 125 (100)		P	Triple negative group; 125 (100)		P	Ki-67 index; 120 (100)			P
	Negative; 69 (55.2)	Positive; 56 (44.8)		Negative; 61 (48.8)	Positive; 64 (51.2)		Negative; 121 (96.8)	Positive; 4 (3.2)		≤ 5%; 25 (20.8)	6 - 19%; 53 (44.2)	≥ 20%; 42 (35.0)	
Negative microcalcifications; 62 (49.6)	29 (23.2)	33 (26.2)	0.060	37 (29.4)	25 (20.00)	0.006	59 (47.2)	3 (2.4)	0.192	16 (13.4)	32 (26.7)	10 (8.3)	0.001
Group 1 (MMG-, USG-); 42 (33.6)	17 (13.6)	25 (20.0)		29 (23.2)	13 (10.4)		39 (31.2)	3 (2.4)		11 (9.2)	24 (20.0)	4 (3.3)	
Group 2 (MMG+, USG-); 20 (16.0)	12 (9.6)	8 (6.4)		8 (6.4)	12 (9.6)		20 (16.0)	0 (0.0)		5 (4.2)	8 (6.7)	6 (5.0)	
Positive microcalcifications													
Group 3 (MMG+, USG+); 63 (50.4)	40 (32.0)	23 (18.4)		24 (19.2)	39 (31.2)		62 (49.6)	1 (0.8)		9 (7.5)	21 (17.5)	32 (26.7)	
Positive microcalcifications; 63 (100)	40 (63.5)	23 (36.5)	0.017	24 (38.1)	39 (61.9)	0.008	62 (98.4)	1 (1.6)	0.438	9 (14.5)	21 (33.9)	32 (50.8)	0.550
Calcifications in a mass; 24 (38.1)	11 (17.5)	13 (20.6)		14 (22.2)	10 (15.9)		23 (36.5)	1 (1.6)		3 (4.8)	9 (14.5)	11 (17.7)	
Calcifications outside a mass; 34 (54.0)	27 (42.9)	7 (11.1)		7 (11.1)	27 (42.9)		34 (54.0)	0 (0.0)		6 (9.7)	9 (14.5)	19 (30.6)	
Intraductal calcifications; 5 (7.9)	2 (3.2)	3 (4.8)		3 (4.8)	2 (3.2)		5 (7.9)	0 (0.0)		0 (0.0)	3 (4.8)	2 (3)	

Abbreviations: MMG-, mammography-negative microcalcifications; MMG+, mammography-positive microcalcifications; USG-, ultrasonography-negative microcalcifications; USG+, ultrasonography-positive microcalcifications; ER-, estrogen receptor; HER2, epidermal growth factor receptor 2.

^a Values are expressed as No. (%).

^b The available number of Ki-67 index was n = 120.

tween MMG and immunohistochemistry. The discrepancy between the findings may be attributed to differences in patient selection, as the mentioned study (3) included DCIS cases with only calcifications on MMG, whereas our study included all DCIS cases with visible or invisible microcalcifications.

In another study, DCIS with microinvasion was associated with a significantly higher Ki-67 index and HER2 ex-

pression and correlated with microcalcifications on USG (30). The Ki-67 index was not correlated with the MMG findings of malignancy, whereas a higher Ki-67 index (≥ 5%) was more frequent in HER2-positive DCIS (3). In the present study, positive microcalcifications on MMG were significantly associated with a high Ki-67 index (≥ 20%). Although masses are the most common USG findings of DCIS, USG can identify 23 to 45% of calcifications found on MMG

(7, 8, 31). In this study, USG showed calcifications in 50.4% of cases. The USG findings of calcifications, distortions, and ductal changes were more significantly associated with a high nuclear grade and comedo necrosis in DCIS (32, 33).

It seems that USG can indicate calcifications more frequently in cases of high-grade DCIS, calcified DCIS (on MMG), and DCIS with comedo necrosis (32). The USG microcalcifications were associated with non-mass lesions, which were in turn correlated with poor prognostic factors, such as a high nuclear grade, comedo necrosis, HER2 positivity, and an increased Ki-67 index (34). The present results showed that visible microcalcifications on USG were associated with a high nuclear grade, comedo necrosis, HER2 positive group, and increased Ki 67 index, these findings are in line with the finding of previous study (32-34).

The present study had some limitations. First, the data were analyzed retrospectively. Second, the sample size was relatively small; the number of samples for each imaging feature was especially small, which might have affected the statistical significance of data. Third, this study focused on pure DCIS showing microcalcifications on MMG and USG, while other features of DCIS on MMG and USG were not compared with the pathological features. Finally, MMC microcalcifications were not evaluated using marker or specimen MMG to determine their correlations with microcalcifications on USG or pathology reports. Therefore, further studies with a prospective design are needed with a large sample size.

In conclusion, DCIS microcalcifications on MMG and USG were correlated with the pathological and immunohistochemical prognostic factors. Microcalcifications detected via imaging were significantly associated with poor prognostic pathological factors such as high nuclear grade and comedo necrosis, as well as poor prognostic biological factors including ER negative group, HER2 positive groups and high Ki-67 index.

Footnotes

Authors' Contribution: Study conception and design, Yun-Woo Chang; Analysis and interpretation of data, Yun-Woo Chang and Eun Ji Lee; Drafting of the manuscript, Yun-Woo Chang; Critical revision of the manuscript for important intellectual content, Yun-Woo Chang; and Statistical analysis, Yun-Woo Chang.

Conflict of Interests: The authors declare no conflict of interest.

Ethical Approval: This retrospective study was approved by the Institutional Review Board (IRB), and the requirement for obtaining informed consent was waived.

Funding/Support: This study was funded by Soonchunhyang University research fund

References

- Allred DC. Ductal carcinoma in situ: Terminology, classification, and natural history. *J Natl Cancer Inst Monogr.* 2010;**2010**(41):134-8. doi: [10.1093/jncimonographs/lgq035](https://doi.org/10.1093/jncimonographs/lgq035). [PubMed: [20956817](https://pubmed.ncbi.nlm.nih.gov/20956817/)]. [PubMed Central: [PMC5161057](https://pubmed.ncbi.nlm.nih.gov/PMC5161057/)].
- Erbas B, Provenzano E, Armes J, Gertig D. The natural history of ductal carcinoma in situ of the breast: a review. *Breast Cancer Res Treat.* 2006;**97**(2):135-44. doi: [10.1007/s10549-005-9101-z](https://doi.org/10.1007/s10549-005-9101-z). [PubMed: [16319971](https://pubmed.ncbi.nlm.nih.gov/16319971/)].
- Bae MS, Moon WK, Chang JM, Cho N, Park SY, Won JK, et al. Mammographic features of calcifications in DCIS: correlation with oestrogen receptor and human epidermal growth factor receptor 2 status. *Eur Radiol.* 2013;**23**(8):2072-8. doi: [10.1007/s00330-013-2827-9](https://doi.org/10.1007/s00330-013-2827-9). [PubMed: [23512196](https://pubmed.ncbi.nlm.nih.gov/23512196/)].
- Burstein HJ, Polyak K, Wong JS, Lester SC, Kaelin CM. Ductal carcinoma in situ of the breast. *N Engl J Med.* 2004;**350**(14):1430-41. doi: [10.1056/NEJMra031301](https://doi.org/10.1056/NEJMra031301). [PubMed: [15070793](https://pubmed.ncbi.nlm.nih.gov/15070793/)].
- Stomper PC, Connolly JL, Meyer JE, Harris JR. Clinically occult ductal carcinoma in situ detected with mammography: analysis of 100 cases with radiologic-pathologic correlation. *Radiology.* 1989;**172**(1):235-41. doi: [10.1148/radiology.172.1.2544922](https://doi.org/10.1148/radiology.172.1.2544922). [PubMed: [2544922](https://pubmed.ncbi.nlm.nih.gov/2544922/)].
- Barreau B, de Mascarel I, Feuga C, MacGrogan G, Dillhuydy MH, Picot V, et al. Mammography of ductal carcinoma in situ of the breast: review of 909 cases with radiographic-pathologic correlations. *Eur J Radiol.* 2005;**54**(1):55-61. doi: [10.1016/j.ejrad.2004.11.019](https://doi.org/10.1016/j.ejrad.2004.11.019). [PubMed: [15797293](https://pubmed.ncbi.nlm.nih.gov/15797293/)].
- Moon WK, Im JG, Koh YH, Noh DY, Park IA. US of mammographically detected clustered microcalcifications. *Radiology.* 2000;**217**(3):849-54. doi: [10.1148/radiology.217.3.r00nv27849](https://doi.org/10.1148/radiology.217.3.r00nv27849). [PubMed: [11110953](https://pubmed.ncbi.nlm.nih.gov/11110953/)].
- Soo MS, Baker JA, Rosen EL. Sonographic detection and sonographically guided biopsy of breast microcalcifications. *AJR Am J Roentgenol.* 2003;**180**(4):941-8. doi: [10.2214/ajr.180.4.1800941](https://doi.org/10.2214/ajr.180.4.1800941). [PubMed: [12646433](https://pubmed.ncbi.nlm.nih.gov/12646433/)].
- Badra FA, Karamouzis MV, Ravazoula P, Likaki-Karatza E, Tzorakoletherakis E, Koukouras D, et al. Non-palpable breast carcinomas: correlation of mammographically detected malignant-appearing microcalcifications and epidermal growth factor receptor (EGFR) family expression. *Cancer Lett.* 2006;**244**(1):34-41. doi: [10.1016/j.canlet.2005.11.047](https://doi.org/10.1016/j.canlet.2005.11.047). [PubMed: [16517064](https://pubmed.ncbi.nlm.nih.gov/16517064/)].
- Rauch GM, Hobbs BP, Kuerer HM, Scoggins ME, Benveniste AP, Park YM, et al. Microcalcifications in 1657 Patients with Pure Ductal Carcinoma in Situ of the Breast: Correlation with Clinical, Histopathologic, Biologic Features, and Local Recurrence. *Ann Surg Oncol.* 2016;**23**(2):482-9. doi: [10.1245/s10434-015-4876-6](https://doi.org/10.1245/s10434-015-4876-6). [PubMed: [26416712](https://pubmed.ncbi.nlm.nih.gov/26416712/)]. [PubMed Central: [PMC5040326](https://pubmed.ncbi.nlm.nih.gov/PMC5040326/)].
- Virnig BA, Tuttle TM, Shamliyan T, Kane RL. Ductal carcinoma in situ of the breast: A systematic review of incidence, treatment, and outcomes. *J Natl Cancer Inst.* 2010;**102**(3):170-8. doi: [10.1093/jnci/djp482](https://doi.org/10.1093/jnci/djp482). [PubMed: [20071685](https://pubmed.ncbi.nlm.nih.gov/20071685/)].
- Bijker N, Peterse JL, Duchateau L, Julien JP, Fentiman IS, Duval C, et al. Risk factors for recurrence and metastasis after breast-conserving therapy for ductal carcinoma-in-situ: Analysis of European Organization for Research and Treatment of Cancer Trial 10853. *J Clin Oncol.* 2001;**19**(8):2263-71. doi: [10.1200/JCO.2001.19.8.2263](https://doi.org/10.1200/JCO.2001.19.8.2263). [PubMed: [11304780](https://pubmed.ncbi.nlm.nih.gov/11304780/)].
- Irshad A, Leddy R, Pisano E, Baker N, Lewis M, Ackerman S, et al. Assessing the role of ultrasound in predicting the biological behavior of breast cancer. *AJR Am J Roentgenol.* 2013;**200**(2):284-90. doi: [10.2214/AJR.12.8781](https://doi.org/10.2214/AJR.12.8781). [PubMed: [23345347](https://pubmed.ncbi.nlm.nih.gov/23345347/)].
- Allred DC, Anderson SJ, Paik S, Wickerham DL, Nagtegaal ID, Swain SM, et al. Adjuvant tamoxifen reduces subsequent breast cancer in women with estrogen receptor-positive ductal carcinoma in situ: A study based on NSABP protocol B-24. *J Clin Oncol.* 2012;**30**(12):1268-73. doi: [10.1200/JCO.2010.34.0141](https://doi.org/10.1200/JCO.2010.34.0141). [PubMed: [22393101](https://pubmed.ncbi.nlm.nih.gov/22393101/)]. [PubMed Central: [PMC3341142](https://pubmed.ncbi.nlm.nih.gov/PMC3341142/)].

15. Polyak K. Molecular markers for the diagnosis and management of ductal carcinoma in situ. *J Natl Cancer Inst Monogr*. 2010;**2010**(41):210-3. doi: [10.1093/jncimonographs/lgq019](https://doi.org/10.1093/jncimonographs/lgq019). [PubMed: [20956832](https://pubmed.ncbi.nlm.nih.gov/20956832/)]. [PubMed Central: [PMC5161056](https://pubmed.ncbi.nlm.nih.gov/PMC5161056/)].
16. Kepple J, Henry-Tillman RS, Klimberg VS, Layeeque R, Siegel E, Westbrook K, et al. The receptor expression pattern in ductal carcinoma in situ predicts recurrence. *Am J Surg*. 2006;**192**(1):68-71. doi: [10.1016/j.amjsurg.2006.04.002](https://doi.org/10.1016/j.amjsurg.2006.04.002). [PubMed: [16769278](https://pubmed.ncbi.nlm.nih.gov/16769278/)].
17. Holmes P, Lloyd J, Chervoneva I, Pequinot E, Cornfield DB, Schwartz GF, et al. Prognostic markers and long-term outcomes in ductal carcinoma in situ of the breast treated with excision alone. *Cancer*. 2011;**117**(16):3650-7. doi: [10.1002/cncr.25942](https://doi.org/10.1002/cncr.25942). [PubMed: [21319154](https://pubmed.ncbi.nlm.nih.gov/21319154/)].
18. Kerlikowske K, Molinaro AM, Gauthier ML, Berman HK, Waldman F, Bennington J, et al. Biomarker expression and risk of subsequent tumors after initial ductal carcinoma in situ diagnosis. *J Natl Cancer Inst*. 2010;**102**(9):627-37. doi: [10.1093/jnci/djq101](https://doi.org/10.1093/jnci/djq101). [PubMed: [20427430](https://pubmed.ncbi.nlm.nih.gov/20427430/)]. [PubMed Central: [PMC2864293](https://pubmed.ncbi.nlm.nih.gov/PMC2864293/)].
19. Rakovitch E, Nofech-Mozes S, Hanna W, Narod S, Thiruchelvam D, Saskin R, et al. HER2/neu and Ki-67 expression predict non-invasive recurrence following breast-conserving therapy for ductal carcinoma in situ. *Br J Cancer*. 2012;**106**(6):1160-5. doi: [10.1038/bjc.2012.41](https://doi.org/10.1038/bjc.2012.41). [PubMed: [22361634](https://pubmed.ncbi.nlm.nih.gov/22361634/)]. [PubMed Central: [PMC3304413](https://pubmed.ncbi.nlm.nih.gov/PMC3304413/)].
20. Tang X, Yamashita T, Hara M, Kumaki N, Tokuda Y, Masuda S. Histopathological characteristics of breast ductal carcinoma in situ and association with imaging findings. *Breast Cancer*. 2016;**23**(3):491-8. doi: [10.1007/s12282-015-0592-0](https://doi.org/10.1007/s12282-015-0592-0). [PubMed: [25644245](https://pubmed.ncbi.nlm.nih.gov/25644245/)].
21. Rauch GM, Kuerer HM, Scoggins ME, Fox PS, Benveniste AP, Park YM, et al. Clinicopathologic, mammographic, and sonographic features in 1,187 patients with pure ductal carcinoma in situ of the breast by estrogen receptor status. *Breast Cancer Res Treat*. 2013;**139**(3):639-47. doi: [10.1007/s10549-013-2598-7](https://doi.org/10.1007/s10549-013-2598-7). [PubMed: [23774990](https://pubmed.ncbi.nlm.nih.gov/23774990/)]. [PubMed Central: [PMC3982796](https://pubmed.ncbi.nlm.nih.gov/PMC3982796/)].
22. Jin ZQ, Lin MY, Hao WQ, Jiang HT, Zhang L, Hu WH, et al. Diagnostic evaluation of ductal carcinoma in situ of the breast: Ultrasonographic, mammographic and histopathologic correlations. *Ultrasound Med Biol*. 2015;**41**(1):47-55. doi: [10.1016/j.ultrasmedbio.2014.09.023](https://doi.org/10.1016/j.ultrasmedbio.2014.09.023). [PubMed: [25479813](https://pubmed.ncbi.nlm.nih.gov/25479813/)].
23. Daniel OK, Lim SM, Kim JH, Park HS, Park S, Kim SI. Preoperative prediction of the size of pure ductal carcinoma in situ using three imaging modalities as compared to histopathological size: Does magnetic resonance imaging add value? *Breast Cancer Res Treat*. 2017;**164**(2):437-44. doi: [10.1007/s10549-017-4252-2](https://doi.org/10.1007/s10549-017-4252-2). [PubMed: [28439735](https://pubmed.ncbi.nlm.nih.gov/28439735/)].
24. Mendelson E, Berg WA; American College of Radiology. ACR BI-RADS ultrasound. In: D'Orsi CJ, editor. *ACR BI-RADS atlas: Breast imaging reporting and data system; mammography, ultrasound, magnetic resonance imaging, follow-up and outcome monitoring, data dictionary*. Virginia, USA: American College of Radiology; 2013.
25. Hammond ME, Hayes DF, Wolff AC, Mangu PB, Temin S. American society of clinical oncology/college of american pathologists guideline recommendations for immunohistochemical testing of estrogen and progesterone receptors in breast cancer. *J Oncol Pract*. 2010;**6**(4):195-7. doi: [10.1200/JOP.777003](https://doi.org/10.1200/JOP.777003). [PubMed: [21037871](https://pubmed.ncbi.nlm.nih.gov/21037871/)]. [PubMed Central: [PMC2900870](https://pubmed.ncbi.nlm.nih.gov/PMC2900870/)].
26. Ohlschlegel C, Zahel K, Kradolfer D, Hell M, Jochum W. HER2 genetic heterogeneity in breast carcinoma. *J Clin Pathol*. 2011;**64**(12):1112-6. doi: [10.1136/jclinpath-2011-200265](https://doi.org/10.1136/jclinpath-2011-200265). [PubMed: [22011446](https://pubmed.ncbi.nlm.nih.gov/22011446/)].
27. Goldhirsch A, Winer EP, Coates AS, Gelber RD, Piccart-Gebhart M, Thurlimann B, et al. Personalizing the treatment of women with early breast cancer: Highlights of the St Gallen International Expert Consensus on the Primary Therapy of Early Breast Cancer 2013. *Ann Oncol*. 2013;**24**(9):2206-23. doi: [10.1093/annonc/mdt303](https://doi.org/10.1093/annonc/mdt303). [PubMed: [23917950](https://pubmed.ncbi.nlm.nih.gov/23917950/)]. [PubMed Central: [PMC3755334](https://pubmed.ncbi.nlm.nih.gov/PMC3755334/)].
28. Hannemann J, Velds A, Halfwerk JB, Kreike B, Peterse JL, van de Vijver MJ. Classification of ductal carcinoma in situ by gene expression profiling. *Breast Cancer Res*. 2006;**8**(5):R61. doi: [10.1186/bcr1613](https://doi.org/10.1186/bcr1613). [PubMed: [17069663](https://pubmed.ncbi.nlm.nih.gov/17069663/)]. [PubMed Central: [PMCI779498](https://pubmed.ncbi.nlm.nih.gov/PMCI779498/)].
29. Ikeda DM, Andersson I. Ductal carcinoma in situ: atypical mammographic appearances. *Radiology*. 1989;**172**(3):661-6. doi: [10.1148/radiology.172.3.2549563](https://doi.org/10.1148/radiology.172.3.2549563). [PubMed: [2549563](https://pubmed.ncbi.nlm.nih.gov/2549563/)].
30. Yao JJ, Zhan WW, Chen M, Zhang XX, Zhu Y, Fei XC, et al. Sonographic Features of Ductal Carcinoma In Situ of the Breast With Microinvasion: Correlation With Clinicopathologic Findings and Biomarkers. *J Ultrasound Med*. 2015;**34**(10):1761-8. doi: [10.7863/ultra.15.14.07059](https://doi.org/10.7863/ultra.15.14.07059). [PubMed: [26324758](https://pubmed.ncbi.nlm.nih.gov/26324758/)].
31. Yu PC, Lee YW, Chou FF, Wu SC, Huang CC, Ng SH, et al. Clustered microcalcifications of intermediate concern detected on digital mammography: Ultrasound assessment. *Breast*. 2011;**20**(6):495-500. doi: [10.1016/j.breast.2011.05.003](https://doi.org/10.1016/j.breast.2011.05.003). [PubMed: [21723728](https://pubmed.ncbi.nlm.nih.gov/21723728/)].
32. Scoggins ME, Fox PS, Kuerer HM, Rauch GM, Benveniste AP, Park YM, et al. Correlation between sonographic findings and clinicopathologic and biologic features of pure ductal carcinoma in situ in 691 patients. *AJR Am J Roentgenol*. 2015;**204**(4):878-88. doi: [10.2214/AJR.13.12221](https://doi.org/10.2214/AJR.13.12221). [PubMed: [25794082](https://pubmed.ncbi.nlm.nih.gov/25794082/)].
33. Park JS, Park YM, Kim EK, Kim SJ, Han SS, Lee SJ, et al. Sonographic findings of high-grade and non-high-grade ductal carcinoma in situ of the breast. *J Ultrasound Med*. 2010;**29**(12):1687-97. doi: [10.7863/jum.2010.29.12.1687](https://doi.org/10.7863/jum.2010.29.12.1687). [PubMed: [21098839](https://pubmed.ncbi.nlm.nih.gov/21098839/)].
34. Cha H, Chang YW, Lee EJ, Hwang JY, Kim HJ, Lee EH, et al. Ultrasonographic features of pure ductal carcinoma in situ of the breast: Correlations with pathologic features and biological markers. *Ultrasonography*. 2018;**37**(4):307-14. doi: [10.14366/usg.17039](https://doi.org/10.14366/usg.17039). [PubMed: [29169230](https://pubmed.ncbi.nlm.nih.gov/29169230/)]. [PubMed Central: [PMC6177689](https://pubmed.ncbi.nlm.nih.gov/PMC6177689/)].